Development of microfabrication process of mesoporous Pt via "Solvent-Evaporation-Mediated Direct Physical Casting": Selective deposition into sloped microchannels

ARTICLE *in* SCIENCE AND TECHNOLOGY OF ADVANCED MATERIALS · JULY 2006

Impact Factor: 3.51 · DOI: 10.1016/j.stam.2006.05.004

Development of microfabrication process of mesoporous Pt via "*Solvent-Evaporation-Mediated Direct Physical Casting*": Selective deposition into sloped microchannels

2006 Sci. Technol. Adv. Mater. 7 438

(http://iopscience.iop.org/1468-6996/7/5/A05)

Available online at www.sciencedirect.com
ScienceDirect
Science and Technology of Advanced Materials 7 (2006) 438–445
SCIENCE AND TECHNOLOGY OF ADVANCED MATERIALS
www.elsevier.com/locate/stam

Development of microfabrication process of mesoporous Pt via "*Solvent-Evaporation-Mediated Direct Physical Casting*": Selective deposition into sloped microchannels

Yusuke Yamauchi[a,b], Hiroki Kitoh[b], Toshiyuki Momma[b,c,*,1], Tetsuya Osaka[a,b,d,1,*], Kazuyuki Kuroda[a,b,c,d,1,*]

[a]*Department of Applied Chemistry, School of Science and Engineering, Waseda University, Ohkubo 3-4-1, Shinjuku-ku, Tokyo 169-8555, Japan*
[b]*Major in Nanoscience & Nanoengineering and Applied Chemistry, Graduate School of Science & Engineering, Waseda University, Ohkubo 3-4-1, Shinjuku-ku, Tokyo 169-8555, Japan*
[c]*CREST, Japan Science & Technology Agency (JST), Honcho 4-1-8, Kawaguchi-shi, Saitama 332-0012, Japan*
[d]*Kagami Memorial Laboratory for Materials Science & Technology, Waseda University, Nishi-waseda 2-8-26, Shinjuku-ku, Tokyo 169-0051, Japan*

Received 27 December 2005; received in revised form 6 May 2006; accepted 8 May 2006
Available online 18 July 2006

Abstract

We have developed an excellent process for selective deposition of mesoporous Pt through tailored microfabrication steps via the "*Solvent-Evaporation-mediated Direct Physical Casting* (SEDPC)" method. The direct observation by high-resolution scanning microscopy (HR-SEM) shows the formation of an ordered mesoporous structure in a very confined area. The cyclic voltammogram of the mesoporous Pt reveals a typical feature of Pt surface. The surface morphology and ordering of the mesostructure strongly depend on the electrodeposition conditions (constant-current and constant-potential depositions). The roughness factors are greatly enhanced as the charge densities in the constant-current deposition are increased. These findings are important for the morphological design of mesoporous metals in a micrometer scale.

Keywords: Mesoporous metal; Mesoporous material; Lyotropic liquid crystal; Platinum; Electroplating; Electrodeposition; Electrocatalyst; Microchannel; Lithography; Microfabrication

1. Introduction

Since the discovery of mesoporous silica (designated later as KSW-1) from layered polysilicate kanemite in 1990 [1], mesoporous molecular sieves prepared through self-assemblies of surfactants have opened many possibilities in the field of advanced materials. The research area covers synthesis [2], structural characterization [3], morphological control (e.g., film, fiber, and monolith) [4], alignment control of mesochannels [5], and so on. The compositions of pore walls have been expanded into not only silica, but also carbon [6], hybrid organosilica [7], metals, etc. In particular, mesoporous metals are of great importance for new developments of many applications including electronic devices, magnetic devices, metal catalysts, and so on.

Mesoporous metals have mainly been prepared by two approaches as follows. One approach is the replication using mesoporous silica as a hard-template. Nanoporous Pt with three-dimensionally ordered networks can be obtained from MCM-48 (*Ia-3d*) [8]. Using SBA-15 (*p6mm*), the interconnection of hexagonally packed Pt nanowires by small bridges is due to the small tunnels between main mesochannels [9]. Isolated metallic nanowires and nanoparticles are also synthesized by the replication method using FSM-16 (*p6mm*), MCM-41

*Corresponding authors. Graduate School of Science & Engineering, Waseda University, Ohkubo 3-4-1, Shinjuku-ku, Tokyo 169-8555, Japan. Tel./fax: +81 3 5286 8309 (T. Momma); Tel.: +81 3 5286 3202; fax: +81 3 3205 2074 (T. Osaka); Tel./fax: +81 3 5286 3199 (K. Kuroda).
E-mail addresses: momma@waseda.jp (T. Momma), osakatet@waseda.jp (T. Osaka), kuroda@waseda.jp (K. Kuroda).
[1]These coauthors contribute equally to this work.

1468-6996/$ - see front matter © 2006 NIMS and Elsevier Ltd. All rights reserved.
doi:10.1016/j.stam.2006.05.004

(*p6mm*), and HMM-1 (*p6mm*) [10]. However, the metals prepared in this method (e.g., Au, Pt, and Ag) are limited to those inactive to dissolution agents (HF or NaOH).

We have focused on another approach of "*Direct Physical Casting*" by the use of lyotropic liquid crystalline (LLC) phase made of nonionic surfactants at high concentrations [11]. This simple one-pot process, proposed initially by Attard et al. [12] can be readily applied to a wide range of metals, which are generally known to be deposited by using reducing agents. Mesoporous metals with various compositions have been reported up to date. We have adopted this concept to prepare mesoporous Ni [13], Pt [14], and Pt–Ni particles [15], mesostructured Ni–Co particles [16], and mesoporous Pt thin films [17] with improved orderings of the mesostructures.

In the previous direct physical casting system, the use of LLC has been limited to the production of planar films and particles. A next challenging issue is the morphological design of mesoporous metals in a micrometer scale. From the viewpoint of miniaturization in microelectronics, microfabrication is very important for the production of more advanced functional nanoscale devices (e.g., highly sensitive microchip reactors, miniaturized sensors, microelectric devices, etc.). Very recently, we have proposed a novel convenient pathway via "*Solvent-Evaporation-mediated Direct Physical Casting* (SEDPC)" for the microfabrication of mesoporous metals [18]. This SEDPC method is basically composed of two steps: (1) the formation of LLC templating mixtures by solvent evaporation and (2) the metal deposition in the presence of LLC. Initially, a precursor solution including metal species, water, surfactant, and ethanol is introduced into a very confined area due to the capillary force. After the volatile solvent is preferentially evaporated, a LLC templating mixture is formed. Then, metal species in the medium are reduced by electrodeposition. In the present work, we have extended the SEPDC method to microfabrication of mesoporous Pt films onto a different type of sloped microchannels. Moreover, we report the effects of the electrodeposition conditions on the ordering, morphology, and roughness factor of mesoporous Pt deposited inside the microchannels. Our processes reported here will be important for rapid production of functional nanoscale devices and novel nanomaterials utilizing mesoporous metals.

2. Experimental

2.1. Starting materials

Non-ionic surfactant ($C_{16}H_{33}(OCH_2CH_2)_8OH$, Aldrich) was used to form LLC. Platinum (IV) chloride hexahydrate ($H_2PtCl_6 \cdot 6H_2O > 98.5\%$, Kanto Kagaku Co.) was used as a Pt source. Ethanol (H_2O content $< 0.005\%$, Wako Chemical Co.) was used both for dilution of precursors and for the removal of templates.

2.2. Selective deposition of mesoporous Pt inside a sloped microchannel

The fabrication of sloped microchannels onto a Si substrate was performed through a series of fabrication steps according to our previous report (Fig. 1, step a–f) [19]. Two patterned microchannels running parallel in the same direction were prepared on a Si substrate where the top and bottom widths were 100 and 30 μm, respectively, and the depth was 50 μm. Firstly, a photoresist was uniformly coated on the Si substrate by spray coating (step g), and then the photoresists on both channels were removed by lithography (step h). Because Si is non-conductive, a current collector was needed for the Pt deposition. Ti and Au for current collectors were uniformly coated onto the Si substrate by vacuum deposition (step i). In this step, a 20 nm titanium layer was firstly deposited on the Si substrate in an ULVAC CRTM-6000 electron beam evaporation chamber, and then a 100 nm gold layer was deposited onto the Ti layer. The presence of the Ti layer promotes the adhesion between the gold and silicon dioxide. After lifting off the photoresist, the Au/Ti layered current collectors were formed onto the channels (step j).

Three processes of substrate preparation were compared for the successful deposition of mesoporous Pt only inside the sloped channels (Fig. 2).

Process A: Firstly, AZP4620 resist (Clariant Japan K.K.), being stable in ethanol, was uniformly coated on a Si substrate by spray coating. Then, the resist only on the microchannels was removed by lithography.

Process B: Firstly, a SiO_2 layer was uniformly formed by a TEOS-CVD method. Secondary, a photoresist was uniformly coated on the Si substrate by spray coating, and then the photoresist only on the microchannels was

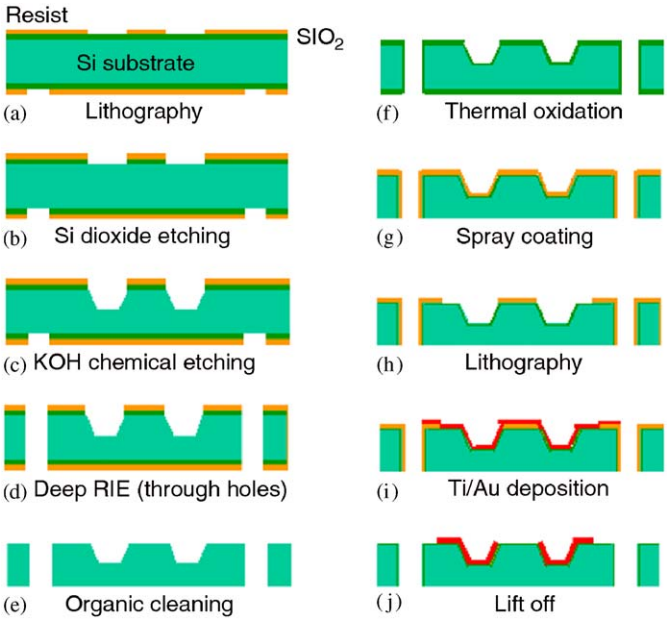

Fig. 1. Schematic procedure of the sloped microchannels on Si substrate.

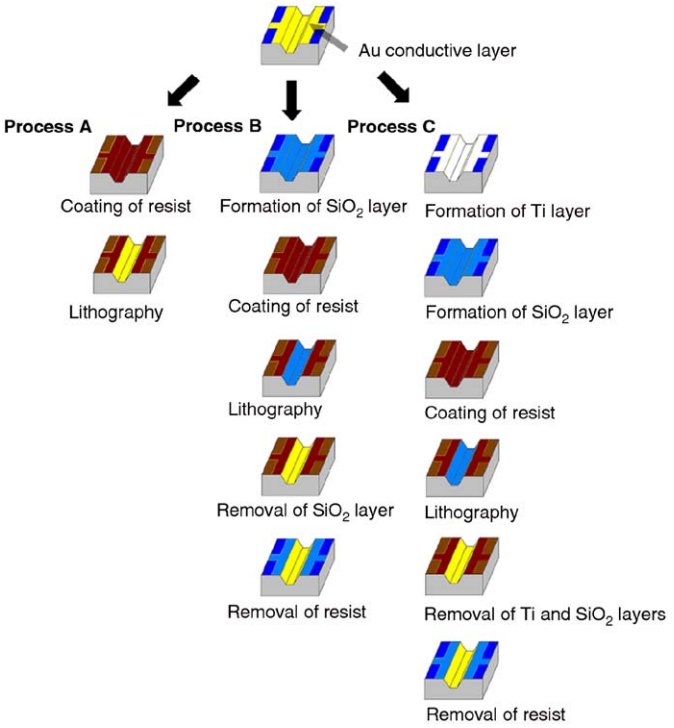

Fig. 2. Three types of substrate fabrications processes for selective deposition of mesoporous Pt.

removed by lithography. Finally, the SiO_2 layer inside the microchannels was removed by NaOH etching, and then the photoresist on the bank was completely removed.

Process C: This procedure was basically same as Process B. The different point was that the 20 nm titanium layer was deposited between gold and silicon dioxide to promote the adhesion between the layers.

Then, a precursor solution with low-viscosity was introduced into the sloped channels by capillary force. A precursor solution as a LLC former was prepared by mixing distilled water (0.29 g), non-ionic surfactant $C_{16}EO_8$ (0.42 g), hydrogen hexachloroplatinate hydrate (0.29 g), and ethanol. After ethanol was preferentially evaporated, the LLC including Pt complexes was entirely formed inside the channels. During the Pt electrodeposition step in the presence of LLC, mesostructured Pt was deposited only on the Au surface inside the microchannel. The electrodeposition was carried out at a constant current by using a HZ-3000 1510 M potentiostat/galvanostat (Hokuto Denko Corp.). A Au-coated Si substrate was used as a counter electrode, and a Ag/AgCl electrode was used as a reference electrode, respectively. The counter electrode was adhered onto LLC to sandwich the LLC. The electrode separation between the working and counter electrodes was fixed to be 400 μm by using a polytetrafluoroethylene (PTFE) separator. Also, the reference electrode was connected to LLC by using a salt-bridge. After deposition, the mesostructured platinum film was immersed in ethanol for 2 d to extract $C_{16}EO_8$. During the removal step, fresh ethanol was replaced 3–4 times and finally washed with deionized water. Energy-dispersive X-ray spectroscopy (EDX) analysis proved less than 3 wt% carbon content and no chlorides in the films, indicating a large amount of surfactants were removed by washing the films with ethanol and water.

After the removal of LLC, the resist (Process A), the SiO_2 layers (Process B), and the SiO_2 layers and Ti layer (Process C) were removed to recover the Au surface on the outside of microchannels (bank) by treating those substrates by lithography (Process A) and alkali-etching (Processes B and C).

2.3. Characterization

High-resolution scanning electron micrographs (HR-SEM) without any additional metal coating were observed with Hitachi S-5200 and S-5500 scanning electron microscopes (SEM) using an accelerating voltage of 20 kV. The Pt deposition on the substrates was confirmed by an Olympus BX-51 optical microscope, and the images were recorded on a digital camera.

3. Results and discussion

3.1. Selective deposition of mesoporous Pt into the sloped microchannels

Three processes are compared for the selective deposition of mesoporous Pt. The advantageous and disadvantageous points of the three processes are as follows. In this section, the electrochemical deposition was carried out by a constant current at 0.1 mA cm^{-2} for 11 h.

Process A is a simple process using an AZP4620 resist. Fig. 3 shows the optical microscopic (OM) and SEM images of the microchannels after the Pt deposition. From the OM image, it seems that Pt was deposited only inside the microchannels (Fig. 3A(1)). However, the SEM images show that Pt was deposited only partly (Fig. 3A(2,3)). The partly remaining resist may prevent the uniform Pt deposition.

In the Process B, the patterned SiO_2 layer was applied as the mask during the Pt deposition. The SiO_2 layer was coated onto the Au layer, and the patterned SiO_2 layers (remaining at the bank only) were prepared by lithography though the silica layers were removed after the deposition. Therefore, it is expected that the Au surface is perfectly exposed to air. The OM and SEM images show that Pt was uniformly deposited inside the microchannels (Fig. 3B(1) and (2)). The OM image also shows the color change into black due to the Pt formation. However, from both the OM and SEM images, it is confirmed that some Pt was also deposited on the outside of the microchannels (Fig. 3B(3)). The precursor solution with low viscosity may interpenetrate between the SiO_2 and Au layers because of their low adhesion. This result suggests that the adhesion between the SiO_2 and Au layers should be improved.

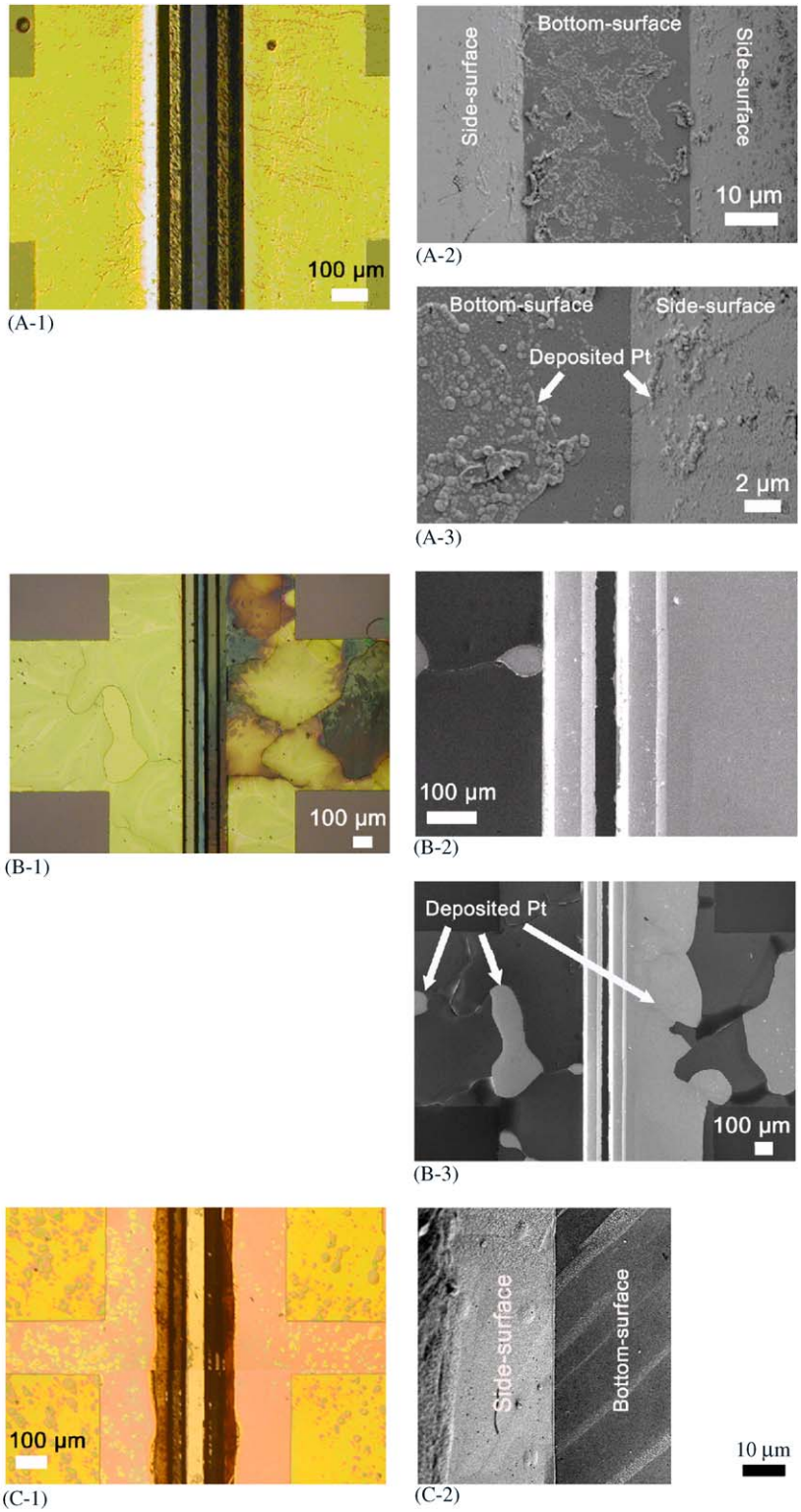

Fig. 3. OM (A-1, B-1, and C-1) and SEM (A-2, B-2, -3, and C-2) images after the Pt deposition. (A: Process A, B: Process B, and C: Process C).

In the Process C, the Ti layer is introduced between the SiO_2 and Au. In the OM image, the color of the microchannels changed into black (Fig. 3C(1)). The OM and SEM images show that Pt is uniformly deposited only onto the Au conductive layer inside the microchannels (Fig. 3C). The EDX data evidently show that Pt can be entirely deposited inside the microchannels, but that no Pt is deposited outside the microchannels (not shown). Consequently, the use of the patterned SiO_2 and Ti layers is the excellent combination for the selective deposition, because the combined layers are highly stable to the precursor solutions.

3.2. Structural characterizations (film morphology and mesostructure)

Fig. 4 shows the birds-eye and cross-sectional views of mesoporous Pt prepared by the Process C. A constant-current deposition at 0.09 mA cm^{-2} for 11 h was applied for the Pt deposition. Fig. 4a represents that Pt is successfully deposited only onto the Au layer inside the microchannels. Even at the interface between the side- and bottom-surfaces, Pt can be deposited without holes (Fig. 4b). The thickness of the Pt film on the bottom- and side-surfaces is around 100–200 nm (Fig. 4c,d). The Pt film is adhered to the substrate. The film thickness is controllable by the electrodeposition time. The formation of continuous films is achievable through the complete filling of the LLC templating mixture.

The formation of the mesoporous Pt structure inside the microchannels is confirmed by HR-SEM. The direct observation by HR-SEM has many advantages over TEM for the characterization of the surface structures and external features. Owing to the high electroconductivity of Pt, the porous nanostructure of mesoporous Pt can be directly observed without any additional metal coating. At the bottom-surface in the microchannel, the stripes are running along the substrate in almost all regions. Almost all the mesochannels are aligned parallel to the substrate (Fig. 5a(1)). The distance between the stripes is roughly estimated to be about 7–8 nm.

For comparison, the mesoporous Pt film was deposited at a constant potential (−0.05 V vs. Ag/AgCl) for 70 min. In this case, the mesoporous Pt film has no cracks and the surface is remarkably flat compared to the film obtained by the constant-current deposition (Fig. 5b). The Fourier diffractogram obtained from the HR-SEM image of the mesoporous Pt film in the full 1 μm^2 region shows clear two spots. It is proved that the mesochannels are running in the same direction over the range of 1 μm^2 (Fig. 5b). This macroscopic alignment of mesochannels is ascribable to the LLC media which are composed of crystalline domains on a micrometer scale [13c]. The real "*direct physical casting*" is achieved under the constant-potential deposition [18].

On the other hand, the Fourier diffractogram for the mesoporous Pt films prepared by a constant-current deposition shows no spots (Fig. 5a(1)). The HR-SEM images prove that the mesoporous Pt film is less ordered than that by the constant-potential deposition. Under the constant-current deposition, it is suggested that side reactions such as the evolution of gas occur at the interface between the Au surface and LLC, leading to the disruption of the mesostructure [12b]. Moreover, the generation of gas during the electrodeposition may be related to the occurrence of some cracks in the film (Fig. 5a(2)), resulting in the short coherence length of single mesoporous crystallinity. Therefore, the domain size regarded as single mesoporous crystallinity must be much smaller than expected.

The surface roughnesses of the mesoporous Pt films and conventional Pt black are compared. Pt black was deposited inside the microchannels at 30 mA cm^{-2} for 10 min in 20 mM H_2PtCl_6 solution. The surface and cross-sectional images of the Pt black film are displayed in Fig. 6. The Pt black shows dendritic morphology containing various pores-size from micropore to macropore and the surface is uneven. On the other hand, the mesoporous Pt

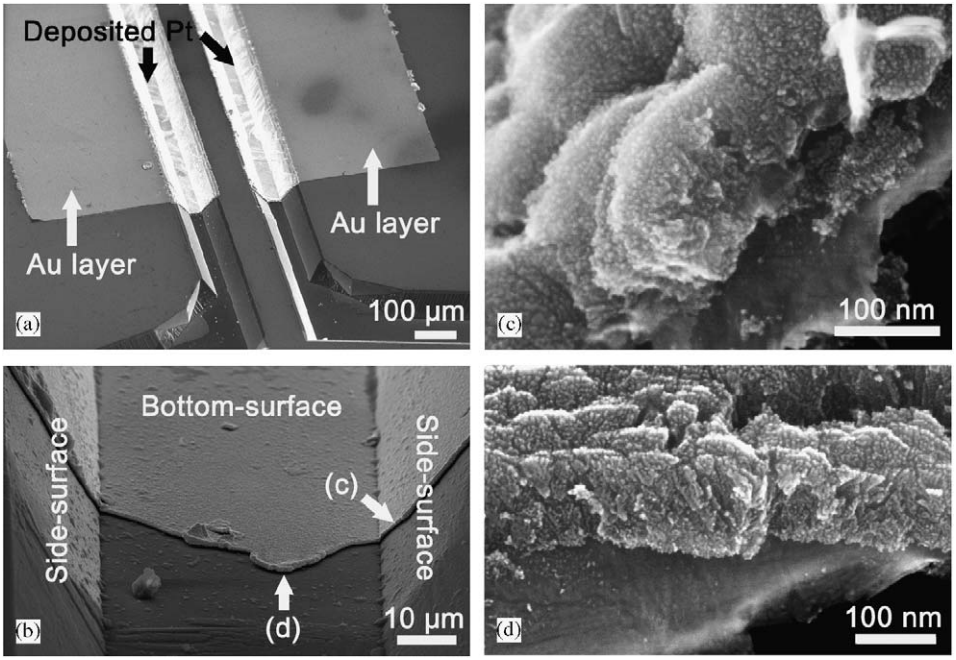

Fig. 4. HR-SEM images: (a) two patterned channels running parallel in the same direction prepared on a Si substrate, (b) entire morphology inside the right microchannels, (c) cross-sectional image of the side-surface in the right microchannel, and (d) cross-sectional image of the bottom-surface in the right microchannel.

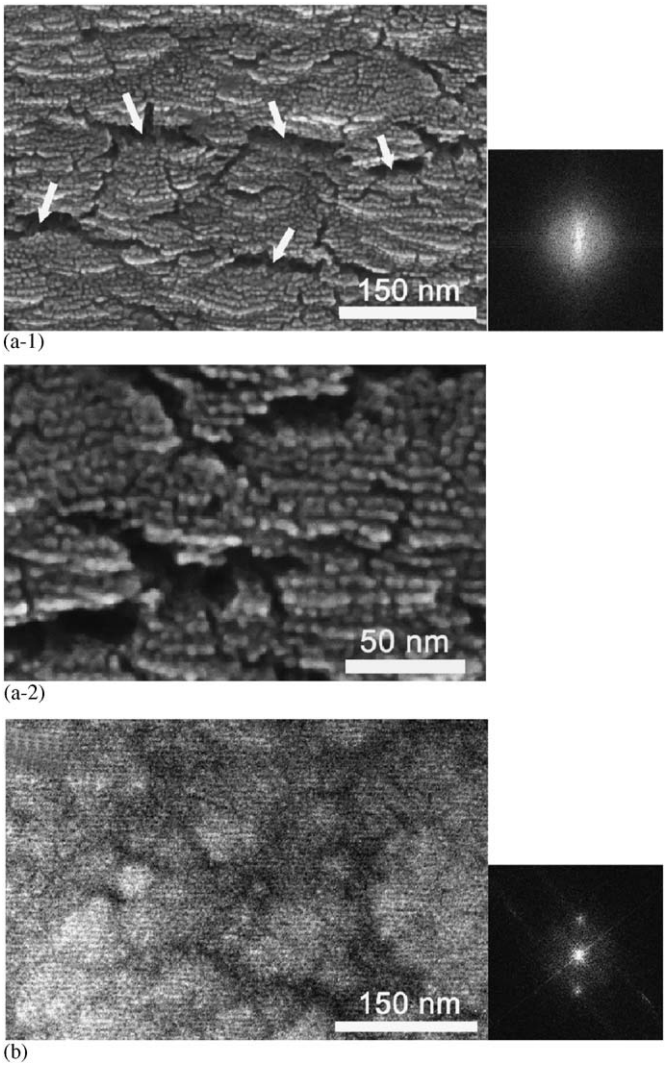

Fig. 5. HR-SEM images and Fourier diffractograms of the bottom-surface inside the right microchannel: (a) mesoporous Pt prepared under the constant-current deposition and (b) mesoporous Pt prepared under the constant-potential deposition. (a-2) is the highly magnified image.

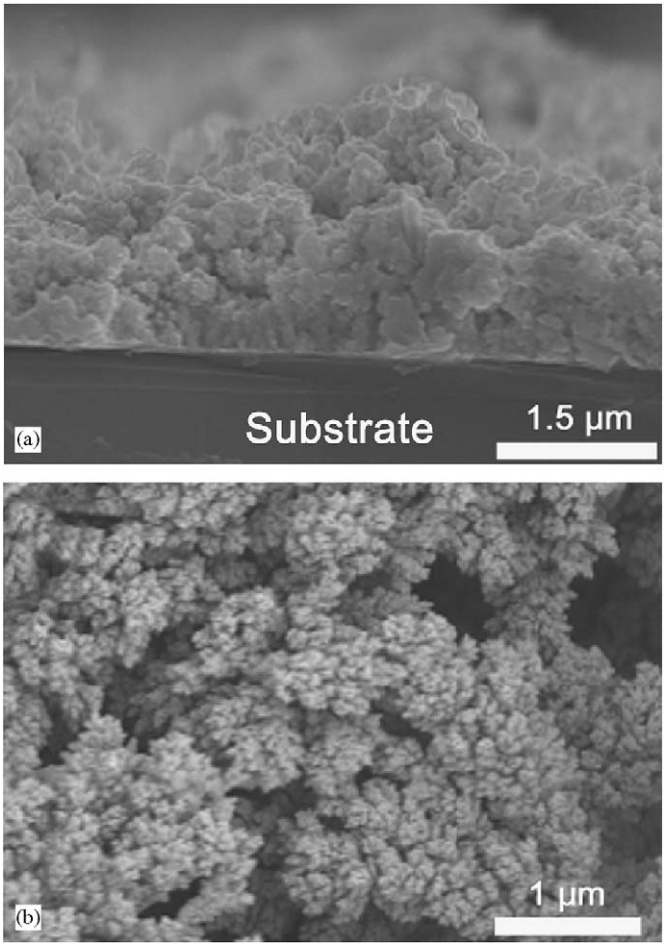

Fig. 6. SEM images of Pt black inside the sloped microchannels: (a) cross-sectional image of the side-surface in the microchannel and (b) the bottom-surface inside the microchannel.

films possess very uniform mesopores. In the general electrodeposition system, it is well known that dendritic structures are often formed on substrates when the plating baths without foreign additives are used. For example, the additives, such as polyethoxylate surfactant and saccharin, inhibit crystal growth, and metal films with smooth surfaces can be prepared. In the present system, the LLC media at highly concentrated surfactants may play a role for making smooth surface [13b].

3.3. Electrochemical performance (CV and roughness factor)

In order to characterize the surface of obtained mesoporous Pt, the electrochemical method was applied because of its merit for proving the catalytic activity of surface. The constant-current densities in the mesoporous Pt deposition were changed from 0.05 to 0.09 mA cm^{-2}. The deposition time for all the samples was 11 h.

The cyclic voltammogram of the mesoporous Pt films (in an aqueous 0.5 M H_2SO_4 solution at 100 mV/s) with the adsorption and desorption of hydrogen show a typical behavior of platinum itself (Fig. 7A). The three anodic peaks at potentials of 0.06, −0.02, and −0.09 V (vs. Ag/AgCl) are consistent with those of the polycrystalline nature of Pt. This result indicates that the surface of the mesoporous Pt works as an electrochemical active area.

From the peak area of hydrogen adsorption, the roughness factors of the mesoporous Pt are calculated with the fact that a monolayer of hydrogen corresponds to 210 μC cm^{-2}. Fig. 7B shows the relationship between the roughness factors and the charge densities in the Pt deposition. The roughness factors are proportional to the charge densities. The calculated plots for an ideal nanostructured system are obtained according to the following assumptions (Fig. 8).

(1) Pore diameter: 3 nm, wall thickness: 4 nm, pore–pore distance: 7 nm.

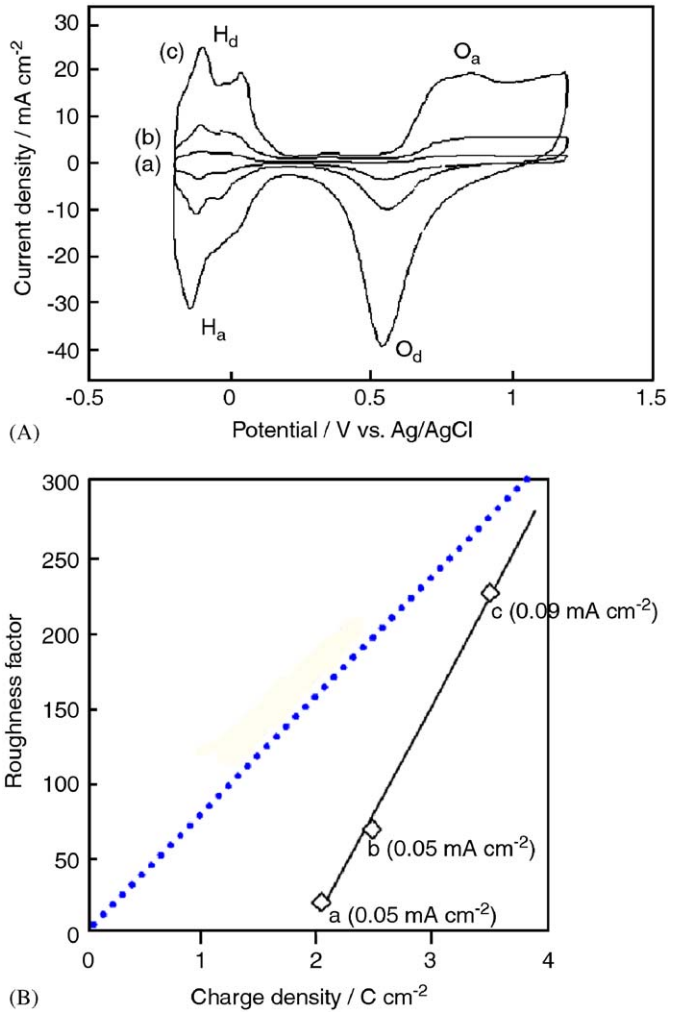

Fig. 7. (A) Cyclic voltammogram for mesoporous Pt in aqueous 0.5 M H_2SO_4 solution at 100 mV/s (H_a: hydrogen adsorption, H_d: hydrogen desorption, O_a: formation of Pt–O, O_d: reduction of Pt oxide). (B) The relationship between the roughness factor and the charges that passed during Pt deposition. The values of the constant-current density during the Pt deposition are denoted respectively. The dotted line is the calculated values of an ideal mesoporous Pt film (Fig. 8).

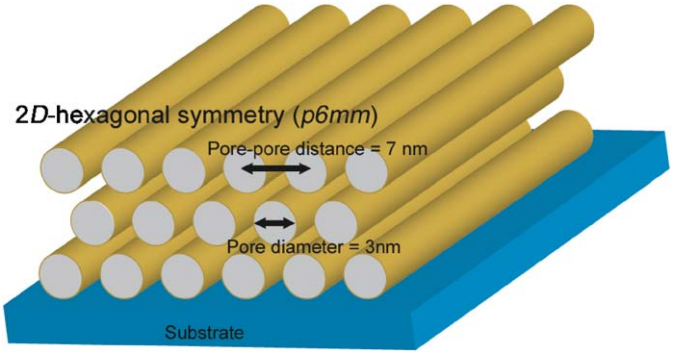

Fig. 8. An ideal mesoporous Pt film.

(2) Mesoporous structure with a 2D-hexagonal symmetry (p6mm). Cylindrical mesochannels were assumed to be aligned parallel to the substrate over the entire area in film.
(3) Straight mesochannels (The surface of the inner mesochannels is very smooth, and has no roughness).
(4) Pt deposition with 100% efficiency. Overall reaction was assumed to proceed as follows:

$$H_2PtCl_6 + 4e^- \rightarrow Pt^0 + 2H^+ + 6Cl^-$$

(The $PtCl_6^{2-}$ species in the presence of LLC are reduced by four electrons through intermediate Pt^{2+} species.)

The observed volumetric surface area for the films is lower than the calculated value (Fig. 7B). This suggests that the mesoporous films contain some portions not accessible by the electrolyte. However, the observed volumetric surface areas approaches to the calculated values as the charge and/or current densities are increased.

The surface morphology and the ordering of the mesostructure are greatly affected by the electrodeposition conditions. As the charge and/or current densities are increased, the mesoporous structures become less perfect and cracks are introduced. The cracks are basically same as those of Fig. 5a. Some cracks in the films may correspond to holes connecting adjacent cylindrical pores. Therefore, even though the mesochannels are aligned parallel to the substrate, the inner walls of pores are more exposed to the electrolyte solution. The HR-SEM image (Fig. 5a(2)) shows that the pore walls of the mesoporous Pt films are composed of connected nanoparticles with an average particle size of ca. 3 nm. The bumpy morphology of the pore walls should contribute to the enhancement of the roughness factor. Even though the surface of the mesoporous Pt films is smooth, the mesoporous Pt possesses a roughness factor similar to that of Pt black. This finding is promising for future applications of this nanomaterial system.

4. Conclusions

We have developed an excellent process for the selective deposition of mesoporous Pt through tailored microfabrication steps. The combination of a resist, SiO_2, and Ti layers during lithography is excellent for making the conductive area for the selective deposition of mesoporous Pt, because the combined layers are highly stable to a precursor solution including ethanol. An important point is that the surface of the mesoporous Pt films with a high roughness factor is very smooth and is adhered to the substrate. We have found that the electrodeposition conditions can lead to significant changes in the surface morphology and the ordering of the mesostructure. The observed volumetric surface area for the films approaches to the value calculated for an ideally nanostructured film as the charge and/or current densities are increased. In the constant-current deposition, some cracks are created in the films, leading to the enhancement of roughness factors. Our novel convenient pathway reported here will be important for the rapid production of functional nanoscale

devices and novel nanomaterials utilizing mesoporous metals. The whole synthetic procedure can be extended to the production of various mesoporous metals and alloys. The macroscopic structural design of mesoporous metals should greatly contribute to practical applications such as micro-sensors, micro-batteries, micro-bioactive materials, miniaturized devices, and so on.

Acknowledgments

The authors greatly appreciate the reviewers' critical comments and corrections. The authors are deeply grateful to Prof. S. Shoji (Department of Electrical Engineering and Bioscience, Waseda University) for helpful comments on a fluid injection system. We would like to thank Dr. S. Motokawa, Mr. M. Sawada, Mr. R. Sebata (Waseda University) for technical supports and discussion on the electrochemical plating and Dr. J. Mizuno (Nanotechnology Laboratory, Waseda University) for suggestions on the fabrication of patterned channels and Prof. Y. Honda (Waseda University) for HR-SEM observation. This work was supported in part by a Grant-in-Aid for Center of Excellence (COE) Research "Molecular Nano-Engineering", the 21st Century COE Program "Practical Nano-Chemistry", and Encouraging Development Strategic Research Centers Program "Establishment of Consolidated Research Institute for Advanced Science and Medical Care" from the Ministry of Education, Culture, Sports, Science and Technology (MEXT), Japanese government. This work is also supported by A3 Foresight Program "Synthesis and Structural Resolution of Novel Mesoporous Materials" from Japan Society for the Promotion of Science (JSPS). One of the present authors (Y.Y.) is grateful for financial supports via a Grant-in Aid for JSPS Fellows from MEXT.

References

[1] T. Yanagisawa, T. Shimizu, K. Kuroda, C. Kato, Bull. Chem. Soc. Jpn. 63 (1990) 988.
[2] (a) C.T. Kresge, M.E. Leonowicz, W.J. Roth, J.C. Vartuli, J.S. Beck, Nature 359 (1992) 710;
(b) D.Y. Zhao, J.L. Feng, Q.S. Huo, N. Melosh, G.H. Fredrickson, B.F. Chmelka, G.D. Stucky, Science 279 (1998) 548.
[3] (a) Y. Sakamoto, M. Kaneda, O. Terasaki, D.Y. Zhao, J.M. Kim, G.D. Stucky, H.J. Shim, R. Ryoo, Nature 408 (2000) 449;
(b) Y. Sakamoto, T.W. Kim, R. Ryoo, O. Terasaki, Angew. Chem. Int. Ed. Engl. 43 (2004) 5231.
[4] (a) M. Ogawa, J. Am. Chem. Soc. 116 (1994) 7941;
(b) H. Yang, A. Kuperman, N. Coombs, S. Mamiche-Afara, G.A. Ozin, Nature 379 (1996) 703;
(c) P.C.A. Alberius, K.L. Frindell, R.C. Hayward, E.J. Kramer, G.D. Stucky, B.F. Chmelka, Chem. Mater. 14 (2002) 3284;
(d) C.W. Wu, T. Aoki, M. Kuwabara, Nanotechnology 15 (2004) 1886.
[5] (a) M. Trau, N. Yao, E. Kim, Y. Xia, G.M. Whitesides, I.A. Aksay, Nature 390 (1997) 674;
(b) H. Miyata, T. Suzuki, A. Fukuoka, T. Sawada, M. Watanabe, T. Noma, K. Takada, T. Mukaide, K. Kuroda, Nature Mater. 3 (2004) 651;
(c) S.H. Tolbert, A. Firouzi, G.D. Stucky, B.F. Chmelka, Science 278 (1997) 264;
(d) K. Kuraoka, Y. Tanaka, M. Yamashita, T. Yazawa, Chem. Commun. (2004) 1198;
(e) Y. Kawashima, M. Nakagawa, T. Seki, K. Ichimura, Chem. Mater. 14 (2002) 2842;
(f) Y. Yamauchi, M. Sawada, T. Noma, H. Ito, S. Furumi, Y. Sakka, K. Kuroda, J. Mater. Chem. 15 (2005) 1137.
[6] S.H. Joo, S.J. Choi, I. Oh, J. Kwak, Z. Liu, O. Terasaki, R. Ryoo, Nature 412 (2001) 169.
[7] S. Inagaki, S. Guan, T. Ohsuna, O. Terasaki, Nature 416 (2002) 304.
[8] H.J. Shin, R. Ryoo, Z. Liu, O. Terasaki, J. Am. Chem. Soc. 123 (2001) 1246.
[9] Z. Liu, O. Terasaki, T. Ohsuna, K. Hiraga, H.J. Shin, R. Ryoo, Chem. Phys. Chem. 2 (2001) 229.
[10] (a) Z. Liu, Y. Sakamoto, T. Ohsuna, K. Hiraga, O. Terasaki, C.H. Ko, H.J. Shin, R. Ryoo, Angew. Chem. Int. Ed. 39 (2000) 3107;
(b) A. Fukuoka, H. Araki, J. Kimura, Y. Sakamoto, T. Higuchi, N. Sugimoto, S. Inagaki, M. Ichikawa, J. Mater. Chem. 14 (2004) 752;
(c) A. Fukuoka, Y. Sakamoto, S. Guan, S. Inagaki, N. Sugimoto, Y. Fukushima, K. Hirahara, S. Iijima, M. Ichikawa, J. Am. Chem. Soc. 123 (2001) 3373.
[11] G.S. Attard, C.G. Göltner, J.M. Corker, S. Henke, R.H. Templer, Angew. Chem. Int. Ed. Engl. 36 (1997) 1315.
[12] (a) G.S. Attard, P.N. Bartlett, N.R.B. Coleman, J.M. Elliott, J.R. Owen, J.H. Wang, Science 278 (1997) 838;
(b) J.M. Elliott, G.S. Attard, P.N. Bartlett, N.R.B. Coleman, D.A.S. Merckel, J.R. Owen, Chem. Mater. 11 (1999) 3602;
(c) A.H. Whitehead, J.M. Elliott, J.R. Owen, G.S. Attard, Chem. Commun. (1999) 331;
(d) I. Nandhakumar, J.M. Elliott, G.S. Attard, Chem. Mater. 13 (2001) 3840;
(e) P.N. Bartlett, P.N. Birkin, M.A. Ghanem, P. de Groot, M. Sawicki, J. Electrochem. Soc. 148 (2001) C119;
(f) P.A. Nelson, J.M. Elliot, G.S. Attard, J.R. Owen, Chem. Mater. 14 (2002) 524;
(g) T. Gabriel, I.S. Nandhakumar, G.S. Attard, Electrochem. Commun. 4 (2002) 610;
(h) P.N. Bartlett, J. Marwan, Microporous Mesoporous Mater. 62 (2003) 73;
(i) P.N. Bartlett, J. Marwan, Chem. Mater. 15 (2003) 2962.
[13] (a) Y. Yamauchi, T. Yokoshima, H. Mukaibo, M. Tezuka, T. Shigeno, T. Momma, T. Osaka, K. Kuroda, Chem. Lett. 33 (2004) 542;
(b) Y. Yamauchi, T. Momma, T. Yokoshima, K. Kuroda, T. Osaka, J. Mater. Chem. 15 (2005) 1987;
(c) Y. Yamauchi, T. Yokoshima, T. Momma, T. Osaka, K. Kuroda, Electrochem. Solid-State Lett. 8 (2005) C141.
[14] Y. Yamauchi, T. Momma, M. Fuziwara, S. Sadasivan Nair, T. Ohsuna, O. Terasaki, T. Osaka, K. Kuroda, Chem. Mater. 17 (2005) 6342.
[15] Y. Yamauchi, S. Sadasivan Nair, T. Momma, T. Ohsuna, T. Osaka, K. Kuroda, J. Mater. Chem. 16 (2006) 2229.
[16] (a) Y. Yamauchi, T. Yokoshima, T. Momma, T. Osaka, K. Kuroda, J. Mater. Chem. 14 (2004) 2935;
(b) Y. Yamauchi, S. Sadasivan Nair, T. Yokoshima, T. Momma, T. Osaka, K. Kuroda, Stud. Surf. Sci. Catal. 156 (2005) 457.
[17] Y. Yamauchi, T. Yokoshima, T. Momma, T. Osaka, K. Kuroda, Chem. Lett. 33 (2004) 1576.
[18] Y. Yamauchi, H. Kitoh, T. Momma, T. Osaka, K. Kuroda, Electrochem. Commum. 7 (2005) 1364.
[19] (a) S. Motokawa, M. Mohamedi, T. Momma, S. Shoji, T. Osaka, Electrochem. Commun. 6 (2004) 562;
(b) S. Motokawa, M. Mohamedi, T. Momma, S. Shoji, T. Osaka, Electrochemistry 73 (2005) 346;
(c) S. Motokawa, H. Obata, M. Mohamedi, T. Momma, S. Shoji, T. Osaka, Electrochemistry 73 (2005) 352.